Letter | Editors' Suggestion

Terahertz field driven giant nonlinear phonon response in ferroelectric semiconductor In-doped (Sn,Pb)Te

H. Handa,[1] Y. Okamura,[1,*] R. Yoshimi,[2] A. Tsukazaki,[3] K. S. Takahashi,[2] Y. Tokura,[1,2,4] and Y. Takahashi[1,2,†]

[1]*Department of Applied Physics and Quantum Phase Electronics Center, University of Tokyo, Tokyo 113-8656, Japan*

[2]*RIKEN Center for Emergent Matter Science (CEMS), Wako 351-0198, Japan*

[3]*Institute for Materials Research, Tohoku University, Sendai 980-8577, Japan*

[4]*Tokyo College, University of Tokyo, Tokyo 113-8656, Japan*

(Received 6 June 2023; revised 20 November 2023; accepted 5 January 2024; published 2 February 2024)

We report the large-amplitude coherent soft phonon dynamics dominated by anharmonicity for ferroelectric semiconductor near topological transitions In-doped (Sn,Pb)Te using high-field terahertz spectroscopy. The phonon frequency is dramatically increased through intense terahertz excitation of soft phonons having large dielectric response. The atomic displacement and phonon anharmonicity, which are quantitively retrieved from the field strength dependent response, are the most enhanced near the ferroelectric transition; the displacement is as large as the spontaneous ferroelectric distortion and the anharmonic positional free energy for phonons reaches up to 75% of the total one. The present findings are crucial for nonlinear phononics including terahertz control of emergent topological phases.

DOI: 10.1103/PhysRevB.109.L081102

Elementary excitation is the fundamental concept describing low-energy quasiparticles in crystalline solids, providing a clear understanding of the many physical properties of materials. For example, the quantized lattice vibration, i.e., phonon, is important for transport phenomena and low-energy optical responses [1]. For some phenomena, anharmonicity of phonon arising from the higher-order term of potential surface plays an essential role beyond the harmonic approximation; the structural phase transitions and the thermal conductivity are eminently illustrative of anharmonicity. While the thermal expansion, scattering, and infrared measurements only observe the averaged anharmonicity along all related coordinates, the anharmonicity along the specific coordinate has rarely been examined so far; the direct experimental observation and quantitative theoretical prediction of phonon anharmonicity are still challenging. The recent advance in the generation of intense terahertz field provides another approach to this issue [2–6]. The intense resonant terahertz excitation can generate the large-amplitude lattice vibration reaching anharmonic regime, and the deviation from harmonic response triggers various nonlinear phenomena. The nonlinear spectral information including the shift of vibration frequency reflects the anharmonicity, enabling the quantitative evaluation of positional free energy. Such a transient large lattice deformation also leads to the coherent control of lattice structural and electronic phases [7–11]. The elucidation of phonon dynamics in anharmonic regime provides an insight into these highly nonlinear responses of quantum materials.

Among various phonon modes, the soft transverse optical (TO) phonon directly coupled to the ferroelectric instability is one intriguing target [12,13], because the inherently large dielectric constant exceeding 10^3 in the terahertz region provides the strong interaction with light. Accordingly, the intense terahertz field can create the soft phonon oscillating with large amplitude through the resonant excitation. So far, a few studies on nonlinear coherent soft phonon dynamics have been reported only on the paraelectric $SrTiO_3$ [3,5]. Thus, the fundamental nature such as the impact of ferroelectric transition on the nonlinear response of phonon still remains elusive. In addition, the ferroelectric semimetals provide intriguing states of matter such as the Weyl semimetal state beyond the conventional ferroelectrics [14].

In this work, we show the nonlinear coherent response of the soft phonon in the ferroelectric semiconductor In-doped (Sn,Pb)Te thin film having a variety of topological electronic phases. We focus on the composition near the topological transition with enhanced dielectric response, which is advantageous for pursuing the large phonon response. The resonant excitation of the soft phonon by the intense terahertz field induces the large frequency shift of the phonon, which is the most enhanced near the ferroelectric transition temperature. These nonlinear responses can be well accounted for by considering the equation of motion under the harmonic and quartic anharmonic positional free energy for phonon. This theoretical analysis quantitatively reveals the variation of the positional free energy near the ferroelectric transition and large atomic displacement induced by the terahertz light irradiation.

(Sn,Pb)Te is the well-known IV-VI semiconductor that crystallizes in a rocksalt structure with ferroelectric instability [Fig. 1(a)]. The end compound SnTe shows the ferroelectric transition with the polar distortion along the ⟨111⟩ axes [15–19]. The displacive-type ferroelectric instability causes the softening of TO phonons, which show the frequency

*Corresponding author: okamura@ap.t.u-tokyo.ac.jp

†Corresponding author: youtarou-takahashi@ap.t.u-tokyo.ac.jp

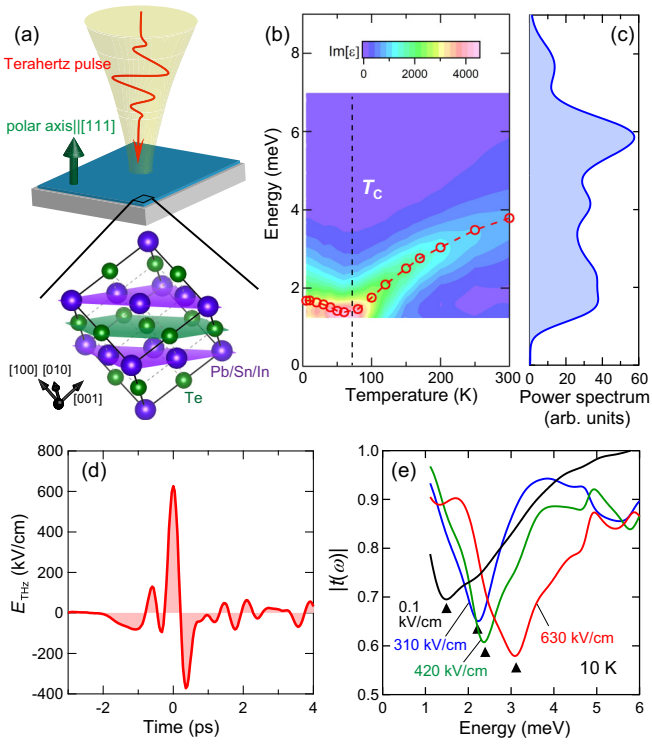

FIG. 1. (a) Crystal structure of (Sn,Pb)Te. (b) Contour map of the imaginary part of the dielectric spectra Im$\varepsilon(\omega)$ in the weak terahertz field limit. The red open circles indicate the phonon energies. The vertical dotted line denotes the ferroelectric transition temperature T_C. (c) The power spectrum of the incident intense terahertz light. (d) The time waveform of the terahertz field. (e) The terahertz field strength dependence of absolute value of complex transmittance, $|t(\omega)|$. The diplike structures are indicated by black triangles for clarity.

lowering towards the ferroelectric transition and one of their displacement patterns is frozen below the transition temperature. These soft TO phonons have noticeably smaller energy (∼2 meV) than the longitudinal optical phonon (∼17 meV). This large longitudinal-transverse splitting enhances the dielectric response, which can be measured by using terahertz spectroscopy even for semimetallic samples with conduction charge [19]. The other end compound PbTe is known as the incipient ferroelectric in bulk form, where the temperature dependence of phonon energy and phonon dispersion have been studied by various techniques, suggesting the strong phonon anharmonicity [20–26]. We also note that this solid solution system shows various topological electronic phases depending on the ferroelectricity and Sn/Pb composition. In between the topological crystalline insulator for SnTe and the trivial insulator for PbTe, the Weyl semimetal state shows up with help of inversion symmetry breaking triggered by the ferroelectric transition [27–31].

We used the high-quality (111)-oriented $(Sn_{0.3}Pb_{0.7})_{0.91}In_{0.09}Te$ epitaxial thin films fabricated on InP(111)A substrate by molecular beam epitaxy [Fig. 1(a); see Supplemental Material Note 1 [32]]. The recent terahertz optical spectroscopy has revealed that the in-plane terahertz response is dominated by the large soft phonon and conduction charge in In-free (Sn,Pb)Te thin films [19]. The ferroelectricity in the epitaxial films is stabilized as compared with the bulk case and the spontaneous polarization points along the out-of-plane direction for all the compositions including PbTe. The dielectric response of soft phonon is enhanced at around the present Sn/Pb ratio (∼3/7) [19], at which the bandgap closing associated with the topological transition is suggested. The 9% indium doping in the present sample tunes the Fermi level position and suppresses the metallic conduction (below the conductivity of $\sim 30\,\Omega^{-1}\,\mathrm{cm}^{-1}$; see Fig. S1 [32]). Accordingly, the charge response due to intraband excitations is negligibly small as compared to the TO soft phonon resonance, whose peak intensity is higher than $\sim 400\,\Omega^{-1}\,\mathrm{cm}^{-1}$, in the terahertz region [Fig. S2 [32]].

The ferroelectric transition and soft phonon dynamics in the linear response regime for the present $(Sn_{0.3}Pb_{0.7})_{0.91}In_{0.09}Te$ film are characterized by using the terahertz time-domain spectroscopy with weak terahertz field excitation. The terahertz light is incident normal to the film plane [Fig. 1(a)] and the peak terahertz field E_{THz} used here is typically ∼0.1 kV/cm (see also Supplemental Material Note 2 [32]). Figure 1(b) shows the imaginary part of the terahertz dielectric spectra, Im$\varepsilon(\omega)$. The clear resonance peak of the TO phonon having in-plane polarization is observed similar to the In-free samples [19]. As the temperature is decreased, this in-plane polarized mode shows substantial softening from 3.8 to 1.5 meV, and subsequently hardening; the phonon energy is determined from the peak energy of Im$\varepsilon(\omega)$. This frequency anomaly is ascribed to the ferroelectric transition with out-of-plane spontaneous polarization as discussed in Ref. [19]; the transition temperature T_C is ∼70 K. Note that, among (almost) degenerated TO soft phonons in the paraelectric pseudocubic phase, only the out-of-plane-polarized mode is eventually frozen below T_C owing to the epitaxial strain. The unfrozen in-plane polarized soft phonons measured in the present study stay below 2 meV, giving rise to the enhanced DC dielectric constant ∼3000 at low temperatures [Fig. S3 [32]]. We note that, as compared to the In-free sample with the same Sn/Pb composition, the $T_C \sim 70$ K and magnitude of dielectric response are almost unchanged by In doping [19].

Having established the linear response, we pursue the nonlinear response. We measure the nonlinear terahertz dielectric spectra by performing the terahertz time-domain spectroscopy under the intense terahertz pulses generated by the tilted-pulse front method [33] (see also Supplemental Material Note 2 [32]). The peak terahertz electric field E_{THz} is 630 kV/cm at maximum and spectral width (1–7 meV) overlaps with resonance energy of the soft phonon in this system [Figs. 1(c) and 1(d)]. We find that the absolute value of complex transmittance spectra, $|t(\omega)|$, strongly depends on the terahertz field strength [Fig. 1(e)]. The diplike structure corresponding to the phonon resonance obviously shifts towards the higher-energy region [black triangles, Fig. 1(e)]. This clear field strength dependent response manifests the deviation from the harmonic approximation in the linear response regime, and accordingly suggests that the coherent oscillation of soft phonon enters the anharmonic regime in higher amplitude of terahertz field. We note that the possible laser-heating effect can be excluded as discussed in Supplemental Material Note 3 [32].

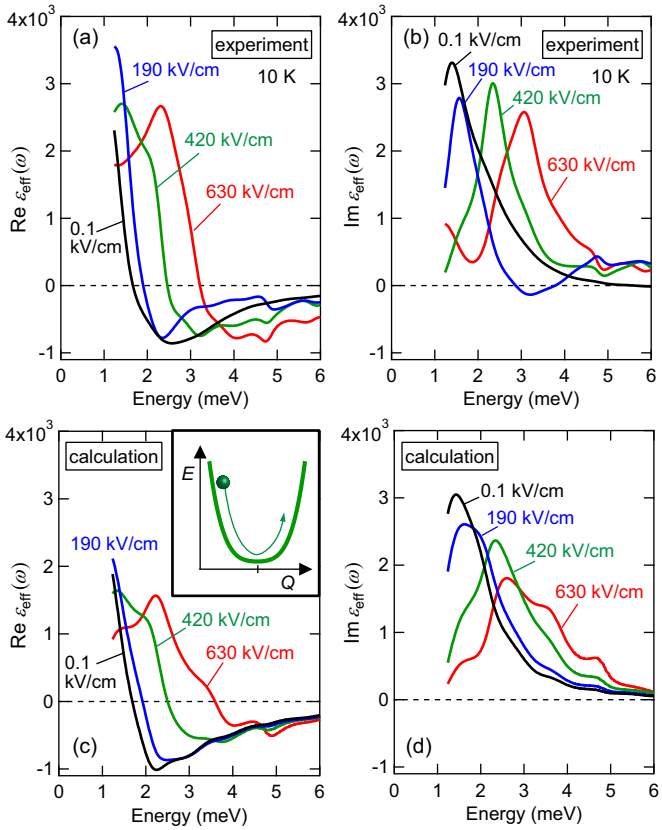

FIG. 2. (a),(b) The real (a) and imaginary (b) parts of effective dielectric spectra $\varepsilon_{\rm eff}(\omega)$ at each peak terahertz field at 10 K. (c),(d) The model calculation of the effective dielectric spectra $\varepsilon_{\rm eff}(\omega)$; the real (c) and imaginary (d) parts. Inset of (c): Schematic illustration of the positional free energy for phonon including the quartic anharmonic term in addition to the harmonic term.

To quantitatively examine this nonlinear response, below we introduce the effective dielectric spectra $\varepsilon_{\rm eff}(\omega)$. This dielectric function is calculated in the same manner as the $\varepsilon(\omega)$ but implicitly includes the field dependent component. In the linear response regime, the phonon resonance shows the dispersive and peak structures in the real and imaginary parts of $\varepsilon(\omega)$, respectively [0.1 kV/cm (black line) in Figs. 2(a) and 2(b); see also Fig. S3(a) [32]]. As the terahertz field strength is increased, this resonance structure shifts towards the high-energy region [Figs. 2(a) and 2(b)]; the resonance energy, the peak in Im $\varepsilon_{\rm eff}(\omega)$ [Fig. 2(b)], is elevated to shift from 1.7 meV for the weak-field limit ($E_{\rm THz} \sim 0.1$ kV/cm) to 3.1 meV for the highest field ($E_{\rm THz} = 630$ kV/cm).

The observed field strength dependent response can be well accounted for by considering the positional free energy for phonon including anharmonicity [Fig. 2(c), inset] [3,5]. Hereafter, we consider the lattice dynamics along the normal mode coordinate Q of soft mode under the temperature dependent positional free energy $V_{\rm ph}$. This is composed of the lowest and second lowest order terms as

$$V_{\rm ph} = \tfrac{1}{2}M^*\omega_T^2\,Q^2 + \tfrac{1}{4}M^*\lambda Q^4.$$

ω_T, M^*, and λ respectively represent the angular frequency of phonon, reduced mass, and quartic anharmonic constant; we used $M^* = 73.7\ m_0$ (m_0: proton mass). The second term represents the quartic anharmonic free energy. Note that, due to the possible existence of randomly distributed 180° rotated or opposite polar multidomains for the present thin film, the in-plane second-order effect arising from the Q^3 term is likely to be canceled out in total and can be omitted (for more details, see also Supplemental Material Note 4 [32]). For the large-amplitude oscillation, this anharmonic term induces the frequency shift. The equation of motion with respect to Q is given by

$$\frac{d^2Q}{dt^2} + \gamma\frac{dQ}{dt} + \omega_T^2 Q + \lambda Q^3 = \frac{Z^* e E_{\rm film}(t)}{M^*},$$

where Z^*, e, t, and $E_{\rm film}(t)$ are the Born effective charge, elementary charge, time, and terahertz electric field inside the film, respectively. We adopted $Z^* = 7.0$, $\omega_T = 1.7$ meV, and $\gamma = 1.6$ meV, which are estimated from the dielectric spectra in the linear response regime. Here, the $E_{\rm film}(t)$ is given as [5]

$$E_{\rm film}(t) = \frac{1}{n_{\rm s}+1}\left(2E_{\rm THz}(t) - \frac{d}{\varepsilon_0 c}\frac{\partial P(t)}{\partial t}\right).$$

The electric polarization $P(t) = 4Z^* eQ/a^3$ ($a \simeq 6.4$ Å: lattice constant [30]) contains four oscillators in a unit cell. $n_{\rm s}$, d, ε_0, and c are refractive index of substrate, film thickness, dielectric constant of vacuum, and speed of light, respectively.

By inputting the experimental terahertz waveform [Fig. 1(d)] into $E_{\rm THz}(t)$, we numerically solve these equations using the Runge-Kutta method and calculate the field strength dependent $\varepsilon_{\rm eff}(\omega)$ from the Fourier transformation of $P(t)$ and $E_{\rm THz}(t)$. The unknown parameter here is the λ in the quartic term, which is determined so as to reproduce the field strength dependent energy shift. The best fit at 10 K is obtained by setting $\lambda = 0.4\,{\rm pm}^{-2}\,{\rm THz}^2$ (Fig. S4 [32]); we also find the good correspondence of spectral characteristics between the experimental and calculated $\varepsilon_{\rm eff}(\omega)$ (Fig. 2). These results clearly demonstrate the essential role of anharmonic free energy for the spectral variation of soft phonon under intense terahertz field. Note that the Born effective charge and damping parameter are assumed to be constants under high terahertz field. Under our experimental conditions, we did not discern a clear signature of such field-induced change of those parameters.

We summarize the terahertz field strength dependence of Im $\varepsilon_{\rm eff}(\omega)$ spectra at each temperature in Figs. 3(a)–3(d). The prominent energy shift is observed for 10 K [Fig. 3(a)] and 80 K [Fig. 3(b)]. As the temperature is increased, we discern the modest energy shift at 150 K [Fig. 3(c)] and the little one at 300 K [Fig. 3(d)]. To examine this temperature dependence quantitatively, we plot the normalized phonon energy shift, which is defined as the resonance energy in the highest field (∼630 kV/cm) divided by that for the linear response regime, in Fig. 3(e). The nonlinear response is the most pronounced at around the $T_{\rm C} \sim 70$ K and mostly suppressed at 300 K, indicating the strong correlation with the ferroelectric instability.

By performing the same numerical analysis shown above, we obtained the temperature variation of the $V_{\rm ph}$ [Figs. 4(a) and 4(b)], which shows the noticeable change with temperature; with decreasing the temperature, the $V_{\rm ph}$ tends to deviate from the harmonic Q^2 dependence and to be dominated by the anharmonic quartic term [Fig. 4(a)]. The anharmonic term (λ)

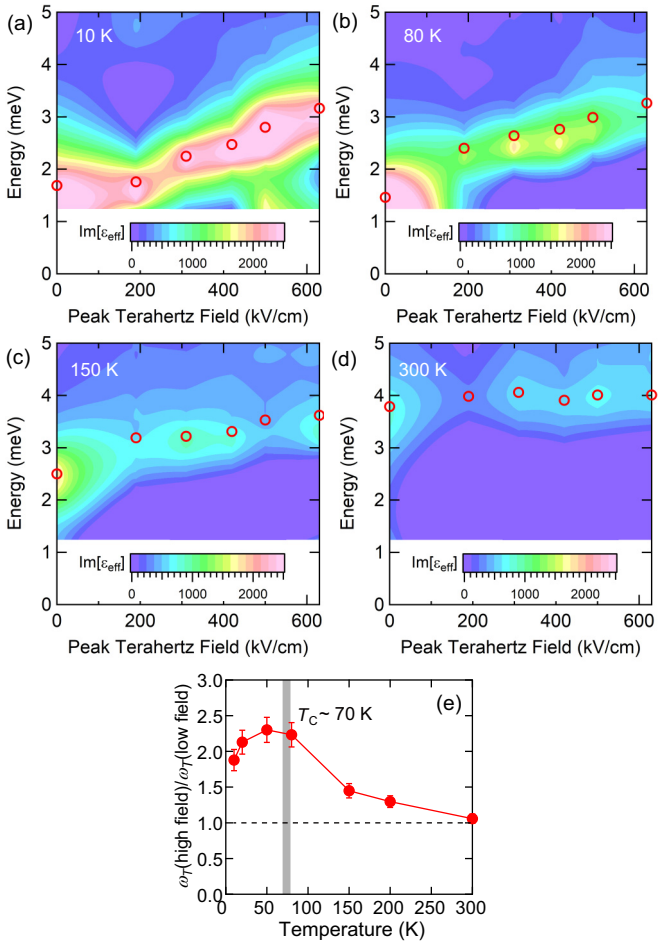

FIG. 3. (a)–(d) Color coded spectra of Im $\varepsilon_{\rm eff}(\omega)$ under strong terahertz field at 10 K (a), 80 K (b), 150 K (c), and 300 K (d). The red open circles represent the resonance energies of the soft phonon. (e) The temperature dependence of the resonance energy at the highest terahertz field ($E_{\rm THz} = 630$ kV/cm) normalized by that at the lowest terahertz field ($E_{\rm THz} \sim 0.1$ kV/cm). The gray bar represents the $T_{\rm C} \sim 70$ K. The error bar represents the statistical error in ten measurements.

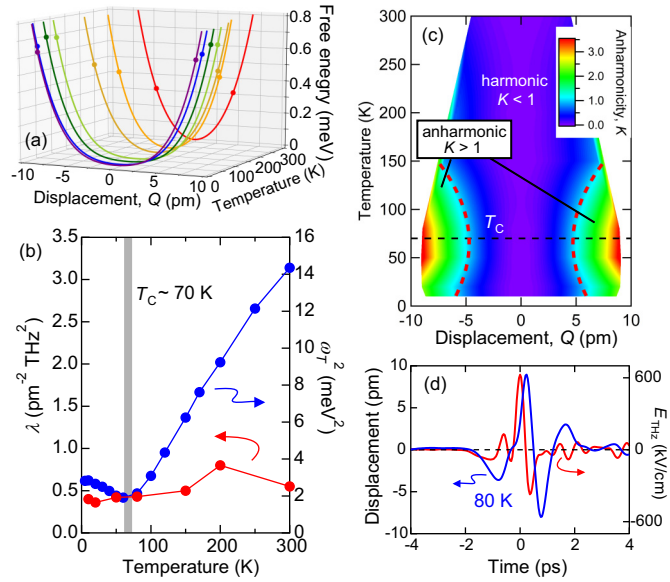

FIG. 4. (a) The positional free energy for phonon retrieved from the effective dielectric spectra. The solid circles represent the maximal displacement induced by the terahertz field. (b) Temperature dependence of ω_T^2 and λ. These are coefficients for the harmonic quadratic and anharmonic quartic terms. (c) The contour map of the anharmonicity K. The colored area is limited to the range of actual displacement Q realized by the highest terahertz field. The red dotted curve shows the boundary between the harmonic and anharmonic regimes, where $K = 1$. The black horizontal dotted line is the ferroelectric transition temperature $T_{\rm C} \sim 70$ K. (d) The time evolution of calculated atomic displacement at 80 K (blue curve) and incident terahertz light field (red curve).

shows weak temperature dependence in contrast to the harmonic term (ω_T^2) [Fig. 4(b)], so that this temperature variation of $V_{\rm ph}$ is almost derived from that of the harmonic term. We map the energy ratio of the quartic anharmonic term to the quadratic harmonic one as $K = \frac{1}{4}M^*\lambda Q^4 / \frac{1}{2}M^*\omega_T^2 Q^2$ on the temperature-Q plane [Fig. 4(c)], in which the colored area is limited to the range of actual displacement Q realized by the highest terahertz field. The anharmonic regime satisfying $K > 1$ is the most enhanced near the $T_{\rm C}$, as indicated by the red dotted curves representing the boundary between the harmonic and anharmonic regimes ($K = 1$). Near $T_{\rm C}$, the anharmonic energy exceeds three times larger than the harmonic one under the highest terahertz field ($K > 3$), indicating that the lattice dynamics is governed by anharmonicity. Thus, the anharmonicity is indispensable to estimate the lattice deformation under the intense terahertz field; it is clearly found that the anharmonic term substantially reduces the amplitude of lattice deformation by comparing the $V_{\rm ph}$ with/without an anharmonic term for the soft mode (solid/dashed line in Fig. S5 [32]). Note that its strong temperature dependence implicitly represents the mode-mode coupling between soft mode and other thermally excited phonons.

The transient change of the nearest-neighbor atomic distance, which is approximately given by Q in the present (slightly rhombohedrally distorted) diatomic rocksalt structure, has a maximum also near the $T_{\rm C}$ [see the solid circles in Fig. 4(a) and the enlarged colored area in Fig. 4(c)]; the largest displacement is 9 pm [Fig. 4(d)], which is 3% of the nearest-neighbor atomic distance (320 pm) and comparable to the ferroelectric distortion in bulk SnTe [16]. The weakened restoring force of the harmonic free energy for soft phonon, which exhibits the enhanced dielectric response, gives rise to such large shift of ions through a resonant terahertz field.

Our present results experimentally reveal the positional free energy along the normal mode coordinate of optical phonon up to quartic term by the high-field terahertz spectroscopy. It is notable that the terahertz field driven displacement observed here is more efficient as compared to the early works for $LiNbO_3$ and $SrTiO_3$ thin film [2,3]. The displacement of 14 pm for oxygen ion is observed for $LiNbO_3$ under the higher terahertz field of 20 MV/cm. For the $SrTiO_3$ film, the displacement of the Ti ion is as small as 1.3 pm for a terahertz field of 880 kV/cm. Thus, the terahertz field induced displacement in our work (9 pm for 630 kV/cm) is in the largest class so far, and the substantially high efficiency for the terahertz field induced coherent lattice deformation

is clearly demonstrated. Also, while the energy fraction of positional free energy for the largest deformation is still dominated by the harmonic term in early works [2,3,5], the quartic anharmonic term dominates 75% of free energy at maximum in the present study [Fig. 4(c)], indicating that the anharmonic term is indispensable for considering the large-amplitude soft mode. These results clearly indicate that the soft mode with strong dielectric response can be utilized for the highly efficient coherent control of lattice especially near the ferroelectric transition point, where the quadratic term takes a minimum.

The insight into the transient lattice deformation under terahertz irradiation will be of crucial importance for realizing the terahertz field induced phononic control of the topological electronic states in the present system [9,10,22]. In PbTe, the lattice deformation induced by the soft phonon is theoretically suggested to induce the change of the direct bandgap at the L point of the Brillouin zone [22]. Therefore, the large atomic displacement observed here can be exploited for the ultrafast control of the band inversion and even of the degeneracy of topological crossing points sensitive to the inversion symmetry breaking [14]. In particular, near the topological transitions, various topological and nontopological phases including Weyl semimetal compete with the subtle balance of relevant parameters [14,28–30], so that dramatic control of the electronic phase would be feasible through the coherent soft phonon excitation.

In conclusion, we have investigated the nonlinear terahertz response derived from the soft phonon excitation in the ferroelectric semiconductor In-doped (Sn,Pb)Te thin film. The direct excitation of the soft phonon using the intense terahertz field induces the dramatic shift of the phonon energy, which is the most enhanced near the T_C. These nonlinear responses can be well accounted for by considering the quartic anharmonicity for the soft phonon. While the nonlinear phonon response attracts much attention in the context of nonlinear phononics in recent years [2–11], the present work demonstrates the coherent phonon dynamics in a fully anharmonic regime. Our findings establish the comprehensive understanding of the soft phonon dynamics including the nonlinear response regime and pave the way for terahertz control of states of matter such as topological electronic phases.

This work was supported by JST Grants No. JPMJFR212X and No. JPMJCR1874 and by JSPS/MEXT Grant-in-Aid for Scientific Research Grants No. 21H01796 and No. 22H04470.

[1] J. M. Ziman, *Principle of the Theory of Solids* (Cambridge University Press, London, 1972).
[2] A. von Hoegen, R. Mankowsky, M. Fechner, M. Forst, and R. Cavalleri, Probing the interaction potential of solids with strong-field nonlinear phononics, Nature (London) **555**, 79 (2018).
[3] M. Kozina, M. Fechner, P. Marsik, T. van Driel, J. M. Glownia, C. Bernhard, M. Radovic, D. Zhu, S. Bonetti, U. Staub, and M. C. Hoffman, Terahertz-driven phonon upconversion in $SrTiO_3$, Nat. Phys. **15**, 387 (2019).
[4] X. Li, T. Qiu, J. Zhang, E. Baldini, J. Lu, A. M. Rappe, and K. A. Nelson, Terahertz-field-induced ferroelectricity in quantum paraelectric $SrTiO_3$, Science **364**, 1079 (2019).
[5] I. Katayama, H. Aoki, J. Takeda, H. Shimosato, M. Ashida, R. Kinjo, I. Kawayama, M. Tonouchi, M. Nagai, and K. Tanaka, Ferroelectric soft mode in a $SrTiO_3$ thin film impulsively driven to the anharmonic regime using intense picosecond terahertz pulses, Phys. Rev. Lett. **108**, 097401 (2012).
[6] R. Mankowsky, A. von Hoegen, M. Forst, and A. Cavalleri, Ultrafast reversal of the ferroelectric polarization, Phys. Rev. Lett. **118**, 197601 (2017).
[7] A. S. Disa, T. F. Nova, and A. Cavalleri, Engineering crystal structures with light, Nat. Phys. **17**, 1087 (2021).
[8] R. Mankowsky, A. Subedi, M. Forst, S. O. Mariager, M. Chollet, H. T. Lemke, J. S. Robinson, J. M. Glownia, M. P. Minitti, A. Frano, M. Fechner, N. A. Spaldin, T. Loew, B. Keimer, A. Georges, and A. Cavalleri, Nonlinear lattice dynamics as a basis for enhanced superconductivity in $YBa_2Cu_3O_{6.5}$, Nature (London) **516**, 71 (2014).
[9] E. J. Sie, C. M. Nyby, C. D. Pemmaraju, S. J. Park, X. Shen, J. Yang, M. C. Hoffmann, B. K. Ofori-Okai, R. Li, A. H. Reid, S. Weathersby, E. Mannebach, N. Finney, D. Rhodes, D. Chenet, A. Antony, L. Balicas, J. Hone, T. P. Devereaux, T. F. Heinz, X. Wang, and A. M. Lindenberg, An ultrafast symmetry switch in a Weyl semimetal, Nature (London) **565**, 61 (2019).
[10] L. Luo, D. Cheng, B. Song, L-L. Wang, C. Vaswani, P. M. Lozano, G. Gu, C. Huang, R. H. J. Kim, Z. Liu, J-M. Park, Y. Yao, K. Ho, I. E. Perakis, Q. Li, and J. Wang, A light-induced phononic symmetry switch and giant dissipationless topological photocurrent in $ZrTe_5$, Nat. Mater. **20**, 329 (2021).
[11] N. Yoshikawa, H. Suganuma, H. Matsuoka, Y. Tanaka, P. Hemme, M. Cazayous, Y. Gallais, M. Nakano, Y. Iwasa, and R. Shimano, Ultrafast switching to an insulating-like metastable state by amplitudon excitation of a charge density wave, Nat. Phys. **17**, 909 (2021).
[12] J. F. Scott, Soft-mode spectroscopy: Experimental studies of structural phase transitions, Rev. Mod. Phys. **46**, 83 (1974).
[13] S. Kamba, Soft-mode spectroscopy of ferroelectrics and multiferroics: A review, APL Mater. **9**, 020704 (2021).
[14] S. Murakami, M. Hirayama, R. Okugawa, and T. Miyake, Emergence of topological semimetals in gap closing in semiconductors without inversion symmetry, Sci. Adv. **3**, e1602680 (2017).
[15] G. S. Pawley, W. Cochran, R. A. Cowley, and G. Dolling, Diatomic ferroelectrics, Phys. Rev. Lett. **17**, 753 (1966).
[16] M. Iizumi, Y. Hamaguchi, K. F. Komatsubara, and Y. Kato, Phase transition in SnTe with low carrier concentration, J. Phys. Soc. Jpn. **38**, 443 (1975).
[17] K. L. I. Kobayashi, Y. Kato, Y. Katayama, and K. F. Komatsubara, Carrier-concentration-dependent phase transition in SnTe, Phys. Rev. Lett. **37**, 772 (1976).
[18] C. D. O'Neill, D. A. Sokolov, A. Hermann, A. Bossak, C. Stock, and A. D. Huxley, Inelastic x-ray investigation of the ferroelectric transition in SnTe, Phys. Rev. B **95**, 144101 (2017).
[19] Y. Okamura, H. Handa, R. Yoshimi, A. Tsukazaki, K. S. Takahashi, M. Kawasaki, Y. Tokura, and Y. Takahashi,

Terahertz lattice and charge dynamics in ferroelectric semiconductor $Sn_xPb_{1-x}Te$, npj Quantum Mater. **7**, 91 (2022).

[20] O. Delaire, J. Ma, K. Marty, A. F. May, M. A. McGuire, M.-H. Du, D. J. Singh, A. Podlesnyak, G. Ehlers, M. D. Lumsden, and B. C. Sales, Giant anharmonic phonon scattering in PbTe, Nat. Mater. **10**, 614 (2011).

[21] E. S. Bozin, C. D. Mallikas, P. Souvatzis, T. Proffen, N. A. Spaldin, M. G. Kanatzidis, and S. J. L. Billinge, Entropically stabilized local dipole formation in lead chalcogenides, Science **330**, 1660 (2010).

[22] M. P. Jiang, M. Trigo, I. Savić, S. Fahy, É. D. Murray, C. Bray, J. Clark, T. Henighan, M. Kozina, M. Chollet, J. M. Glownia, M. C. Hoffmann, D. Zhu, O. Delaire, A. F. May, B. C. Sales, A. M. Lindenberg, P. Zalden, T. Sato, R. Merlin, and D. A. Reis, The origin of incipient ferroelectricity in lead telluride, Nat. Commun. **7**, 12291 (2016).

[23] C. W. Li, O. Hellman, J. Ma, A. F. May, H. B. Cao, X. Chen, A. D. Christianson, G. Ehlers, D. J. Singh, B. C. Sales, and O. Delaire, Phonon self-energy and origin of anomalous neutron scattering spectra in SnTe and PbTe thermoelectrics, Phys. Rev. Lett. **112**, 175501 (2014).

[24] Y. Xia, Revisiting lattice thermal transport in PbTe: The crucial role of quartic anharmonicity, Appl. Phys. Lett. **113**, 073901 (2018).

[25] A. Baydin, F. G. G. Hernandez, M. Rodriguez-Vega, A. K. Okazaki, F. Tay, G. Timothy Noe, I. Katayama, J. Takeda, H. Nojiri, P. H. O. Rappl, E. Abramof, G. A. Fiete, and J. Kono, Magnetic control of soft chiral phonon in PbTe, Phys. Rev. Lett. **128**, 075901 (2022).

[26] G. A. S. Ribeiro, L. Paulatto, R. Bianco, I. Errea, F. Mauri, and M. Calandra, Strong anharmonicity in the phonon spectra of PbTe and SnTe from first principles, Phys. Rev. B **97**, 014306 (2018).

[27] T. H. Hsieh, H. Lin, J. Liu, W. Duan, A. Bansil, and L. Fu, Topological crystalline insulators in the SnTe material class, Nat. Commun. **3**, 982 (2012).

[28] T. Liang, S. Kushwaha, J. Kim, Q. Gibson, J. Lin, N. Kioussis, R. J. Cava, and N. P. Ong, A pressure-induced topological phase with large Berry curvature in $Pb_{1-x}Sn_xTe$, Sci. Adv. **3**, e1602510 (2017).

[29] C. L. Zhang, T. Liang, N. Ogawa, Y. Kaneko, M. Kriener, T. Nakajima, Y. Taguchi, and Y. Tokura, Highly tunable topological system based on PbTe-SnTe binary alloy, Phys. Rev. Mater. **4**, 091201(R) (2020).

[30] R. Yoshimi, M. Masuko, N. Ogawa, M. Kawamura, A. Tsukazaki, K. S. Takahashi, M. Kawasaki, and Y. Tokura, Versatile electronic states in epitaxial thin films of (Sn-Pb-In)Te: From topological crystalline insulator and polar semimetal to superconductor, Phys. Rev. Mater. **5**, 094202 (2021).

[31] C. L. Zhang, T. Liang, M. S. Bahramy, N. Ogawa, V. Kocsis, K. Ueda, Y. Kaneko, M. Kriener, and Y. Tokura, Berry curvature generation detected by Nernst responses in ferroelectric Weyl semimetal, Proc. Natl. Acad. Sci. USA **118**, e2111855118 (2021).

[32] See Supplemental Material at http://link.aps.org/supplemental/10.1103/PhysRevB.109.L081102 for condition of thin film fabrication, terahertz spectroscopy, evaluation of laser-induced heating, theoretical analysis and additional experimental data.

[33] H. Hirori, A. Doi, F. Blanchard, and K. Tanaka, Single-cycle terahertz pulses with amplitudes exceeding 1 MV/cm generated by optical rectification in $LiNbO_3$, Appl. Phys. Lett. **98**, 091106 (2011).